Vygandas Rutkūnas, Agne Gedrimiene, Reinhilde Jacobs, Mangirdas Malinauskas

Comparison of conventional and digital workflows for implant-supported screw-retained zirconia FPD bars: Fit and cement gap evaluation using SEM analysis

KEY WORDS
diagnosis, passive fit, prosthodontics, restorative dentistry

ABSTRACT

Purpose: To assess the fit and cement gap of fixed partial dentures supported by two implants made using conventional and digital workflows.

Materials and methods: Patients requiring fixed partial dentures supported by two implants were included in the study. Forty-eight zirconia fixed partial denture bars supported by two implants were produced using a conventional (n = 24, group C) and digital (n = 24, group D) workflow. All implants (AnyOne, MegaGen, Daegu, Korea) had the same internal connection prosthetic platform. Silicone open tray impressions with splinted copings (group C) and digital impressions using a Trios 3 intraoral scanner (3Shape, Copenhagen, Denmark) (group D) were taken for each patient. The fit and cement gap were assessed by scanning electron microscopy on the verified master cast. The distance between reference points on the titanium base and implant analogue was measured with and without tightening the prosthetic screw. The difference in distance was calculated and represented the misfit (D_{misfit}). The cement gap (D_{cement}) was measured as the shortest vertical distance from the inferior edge of the bar to the top edge of the titanium base.

Results: The median D_{misfit} values (interquartile range) differed significantly ($P < 0.05$) between the groups, with 59 (60) µm for group C and 78 (88) µm for group D. Fixed partial dentures fabricated using a digital workflow presented lower D_{cement} values (35 [26] µm) than in conventional group (38.9 [23] µm) ($P < 0.05$).

Conclusions: Both workflows produced different levels of fit and cement gap when measured on the master casts using scanning electron microscopy. A cast-free digital workflow was associated with a lower cement gap, but larger misfit was detected when measuring on the verified master cast.

Conflict-of-interest statement: *The authors declare there are no conflicts of interest related to this study*.

Introduction

The accuracy of screw-retained implant-supported restorations is critical to the success of dental implant treatment. It is closely associated with the concept of passivity, which several authors have attempted to define[1,2]. Theoretically, passive fit of a screw-retained restoration is achieved when opposing surfaces of the implant and the prosthetic component are in maximal spatial congruency, without strain in the components after the final tightening of all screws[3]. Data regarding technical and biological complications originating from non-passive implant-supported prostheses

exist but are controversial, but complete passivity is virtually impossible to achieve in clinical situations[2,4,5].

The risk of misfit is predetermined during the treatment planning and implant placement stages, as an increased number of implants and increased angulation and distance between them can negatively affect the fit[3]. Distortions in restorative procedures originate with the impression procedure and can potentially grow with each step of the selected workflow. A conventional workflow involving analogue impressions, plaster casts and CAD/CAM to fabricate the framework is usually employed[6]. A digital workflow involving an intraoral scanner (IOS) can eliminate some steps and drawbacks related to the conventional one; however, it also can introduce errors during the digital impression, CAD/CAM and 3D printing procedures. Regardless of the workflow, inaccuracies can still stem from sintering, porcelain firing processes, cementation techniques and the manual skills of the operator. The accuracy of the workflow can differ with implant- and abutment-level prosthodontics and is influenced by various implant–abutment connection types, materials and fabrication methods[7-9].

Different techniques for misfit evaluation are widely discussed in the literature. Microscopic methods such as light microscopy or scanning electron microscopy (SEM) can be used to measure the implant–abutment gap[2]. Misfit can also be assessed through photoelastic stress analysis, strain measurements, finite element modelling, or by making surface superimpositions of the framework and master cast[10]. In clinical conditions, misfit is usually evaluated using techniques including visual inspection, tactile sensation combined with alternate finger pressure, and radiography. The one screw (Sheffield test) and screw resistance tests are considered relatively more accurate[2,3,10].

In a conventional workflow, restorations are cemented to the titanium bases on the plaster casts; however, multiple connections and disconnections of the prosthetic components and the type of implant–abutment connection can contribute to different degrees of abutment malpositioning[11]. This can lead to minor misfit between the restoration and titanium base that can be compensated by the increased cement gap and compromise retention[12].

Restorations created using digital impressions often require 3D printed models for adjustment of restoration contours and porcelain layering. Based on current clinical experience and the limited research data available, the accuracy of 3D printed models is still insufficient for multiple implant-supported restorations[13]. When using a cast-free approach, full-contour restorations can be cemented to titanium bases directly, avoiding the need for 3D printing of the cast and ensuring the best fit between the components[14].

An increasing number of studies are reporting the accuracy of digital implant impressions[15]; however, most of these are in vitro studies and address only the initial step of the digital workflow and thus cannot represent the fit of the final restoration. Moreover, the results of in vitro studies cannot be directly applied clinically. As such, clinical studies using well-defined criteria for fit evaluation and comparing implant-supported FPDs fabricated using conventional and digital workflows are greatly needed.

The aims of this study were as follows:

- to compare clinically the fit of screw-retained zirconia FPD bars supported by two implants, made using conventional and digital workflows;
- to evaluate and compare the fit and cement gap size of FPD bars in a conventional and digital group using SEM measurements on the master cast;
- to estimate the association of distance and angulation between the implants with the fit of FPD bars and cement gap size in both groups.

The null hypotheses were that the fit of the FPD bars and the cement gap size do not differ between conventional and digital workflows implemented in a clinical situation, and that the angulation and distance between implants are not associated with the fit of the FPD bars and the cement gap size.

Materials and methods

Patients requiring FPDs supported by two implants in the posterior region of the dental arch were included in this clinical study. Patients with limited mouth opening, temporomandibular disorders or extremely non-parallel implants, all of which would prevent removal of splinted impression copings, were excluded from the study. The clinical study was conducted in accordance with the standards outlined in the Declaration of Helsinki and was approved by the Vilnius Regional Ethics Committee for Biomedical Research (No 158 200-16-861-370). All patients gave their informed consent to participate. Regardless of diameter, all implants (AnyOne, MegaGen, Daegu, Korea) shared the same prosthetic platform and had an 11-degree internal hex conical connection. There were 14 FPDs supported by two implants in the maxilla and 10 in the mandible. With regard to length, there were seven two-unit, eleven three-unit and six four-unit FPD bars. A total of 48 zirconia FPD bars supported by two implants were produced using conventional (n = 24, group C) and digital (n = 24, group D) workflows. The study workflow is presented in Fig 1. Conventional and digital impressions were taken at the same visit by one operator (VR). Randomisation (https://www.random.org/) was used to determine the order in which the different types of impression would be taken.

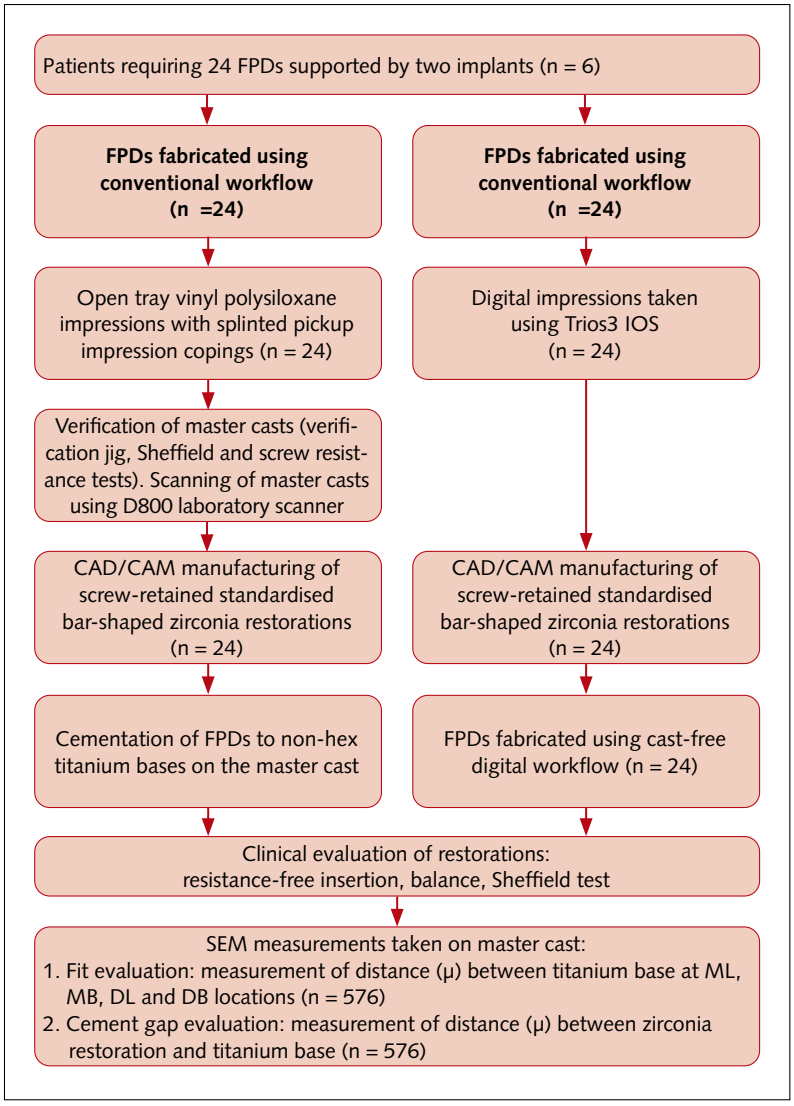

Fig 1 Study workflow.

Conventional workflow

For the conventional workflow, open tray impressions were taken using splinted pickup impression copings (Individo Lux, VOCO, Cuxhaven, Germany) with vinyl–polysiloxane material (Express, 3M, St Paul, MN, USA) and custom-made impression trays (VOCO). The splinting procedure for the impression copings and verification of their passive fit were carried out as described in the literature[16]. Master casts were poured using type IV plaster (FujiRock, GC, Tokyo, Japan) according to the manufacturer's instructions and allowed to set at room temperature for 24 hours. The verification jig (Pattern Resin, GC) was fabricated on the master cast, and the verification procedure was accomplished clinically using a Sheffield and screw resistance test. After the master cast was verified, corresponding scan bodies were secured to the implant analogues with a torque of 15 Ncm, and scanning was done using a laboratory scanner (D800, 3Shape, Copenhagen, Denmark). An experienced dental technician designed the screw-retained bar-shaped restorations (Dental System, 3Shape). They consisted of two cylinders connected with a bar and had a minimal diameter at the gingival level and no contacts to adjacent or opposing teeth. This was done to avoid any additional interference, except contact at

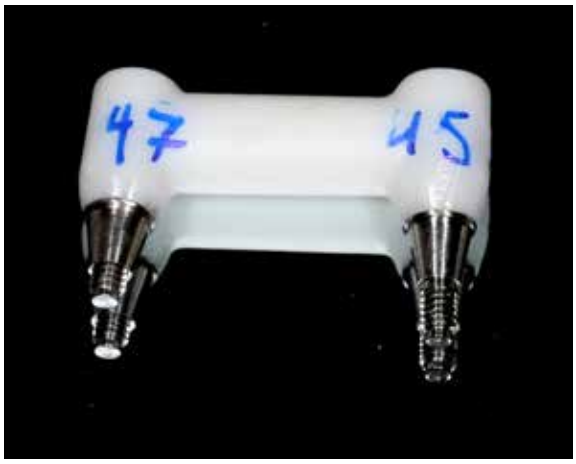

Fig 2 Screw-retained zirconia restoration supported by two implants after cementation to titanium bases.

the implant–abutment connection during evaluation of the fit. The bars were milled from zirconia (KATANA Zirconia HT, Kuraray Noritake Dental, Osaka, Japan) using a five-axis milling machine (VHF S1 Impression, VHF Camfacture, Ammerbuch, Germany). After milling, they were sintered and fitted on the master cast under the microscope (Eschenbach Stereomikroskop 33213, Gelenkarm, Nuremberg, Germany). Airborne-particle abrasion was used on the intaglio surface of the FPDs and bonding surfaces of the titanium bases according to the manufacturers' recommendations. Later, FPD bars were cemented (Multilink Hybrid, Ivoclar Vivadent, Schaan, Liechtenstein) to the original non-hex titanium bases (Ø 4 mm ZrGEN abutment, MegaGen), which were first screwed to the implant analogues on the master cast. Following cementation, the cement access was carefully removed, and the abutment surface was polished and cleaned with alcohol (Fig 2). Twenty-four screw-retained bars were made using a conventional workflow and formed group C.

Digital workflow

In group D, intraoral scanning was performed using the original scan bodies torqued to the implants at 15 Ncm and a Trios 3 IOS (3Shape, version 1.3.4.2). A standardised scanning technique capturing fewer than 1000 images per arch was used. Scanning in the maxilla started from the occlusal surface, and then the buccal and palatal surfaces were captured. In the mandible, the occlusal surface was scanned, followed by the lingual and buccal surfaces. The data were sent to the lab and used for the CAD design of the zirconia bars. The bar shape used for the restoration in the Dental System software and the milling and sintering parameters were the same as those used for group C. After fabrication, the good fit of the titanium base to the zirconia bar was confirmed by a dental technician using a microscope. The technician then cemented the zirconia bars to titanium bases using a cast-free approach, following the same protocol for surface preparation and cement application as in group C. A total of 24 bars were produced using this workflow and formed group D.

Measurements

All zirconia bars in groups C and D were evaluated subjectively for fit (resistance-free insertion, absence of balance, Sheffield test) on the master cast, and intraorally by one blinded operator (VR). No major misfit was detected clinically in either group. After this, all bars were subjected to SEM analysis (TM-1000, Hitachi High-Technologies, Tokyo, Japan) in random order. Before measurements were taken, the master casts were trimmed to ensure that the implant analogue was parallel to the measurement table of the SEM machine. Measurements were performed by a blinded investigator (AG). The screw of the mesial implant was tightened to 35 Ncm and considered as passive, while that of the distal implant was not tightened at all. The distance from the top margin of the titanium base to that of the mesial implant analogue ($D_{passive}$) was measured three times with the implant analogue in four different locations (mesiobuccal [MB], distobuccal [DB], mesiolingual [ML] and distolingual [DL]) at 150× magnification (Fig 3). To standardise the measurement locations, scratch marks were made on the implant analogues using a sharp scalpel. The bar was then removed from the cast and replaced, and the screw on the distal implant abutment was tightened to 15 Ncm. The distance

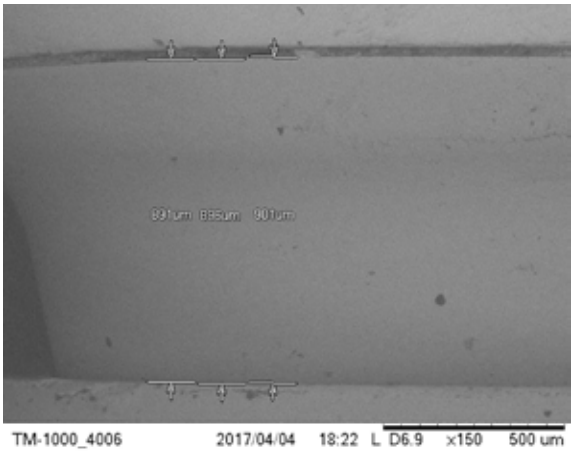

Fig 3 Measurement of distance from titanium base to implant analogue (D_{misfit}) at a standardised location marked with a scratch (×150 magnification).

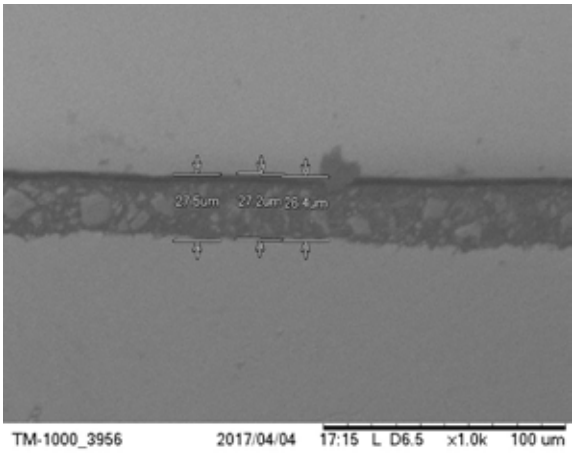

Fig 4 Measurement of D_{cement} using SEM (×1000 magnification).

($D_{non\text{-}passive}$) on the mesial implant analogue was measured in the same way. The same sequence of measurements was completed on the distal implant analogue. A total of 576 measurements were taken using 48 FPD bars. Due to inaccuracies in the SEM images (cement remnants or scratching on the surface causing difficulties in selecting the reference points), three measurements were excluded from further analysis. The difference in distance between the passive and non-passive situation (D_{misfit}) was calculated for each measurement site according to the following formula: $D_{misfit} = D_{non\text{-}passive} - D_{passive}$.

Like the difference between D_{misfit} in each FPD bar in groups C and D, ΔD_{misfit} was calculated and used later to assess its possible associations with interimplant distance and angulation using the following formula: $\Delta D_{misfit} = D_{misfit}$ (group C) – D_{misfit} (group D). Root mean square (RMS) values for D_{misfit} and ΔD_{misfit} were used for further analysis.

The cement gap in groups C and D was evaluated by measuring the shortest vertical distance from the inferior edge of the zirconia bar to the top edge of the titanium base (D_{cement}) (Fig 4). D_{cement} was evaluated at the same MB, DB, ML and DL locations at 1000× magnification. Three measurements were taken at each location. A total of 576 measurements were taken of the cement gap (three measurements were excluded for the aforementioned reasons).

Like the difference in D_{cement} values between groups C and D, ΔD_{cement} was calculated to assess its possible associations with interimplant distance and angulation using the following formula: $\Delta D_{cement} = D_{cement}$ (group C) – D_{cement} (group D). RMS values for D_{cement} and ΔD_{cement} were used for further analysis.

The effect of interimplant distance and angulation on the fit of the bars and cement gap was estimated. For this reason, distances between and angulation of implants were calculated using standard tessellation language (STL) files produced from digital impressions (group D) and scanned master casts (group C). STL files and CAD casts of scan bodies were imported and registered using a modified iterative closest point algorithm in reverse engineering software (Rapidform 2006, INUS Technology, Seoul, Korea). The distance between and angulation of scan bodies were measured for groups C and D. The centre point of the scan body was chosen as the intersection between a selected centre axis and top plane of the scan body. The distance between the centre points of the two scan bodies was measured. The angulation of the scan bodies was measured as the angle between two vectors representing the axes of the scan bodies in 3D space (Fig 5). The mean linear and angular parameters were calculated using the following formula: (D800 data + Trios3 data)/2. The distance and angulation data

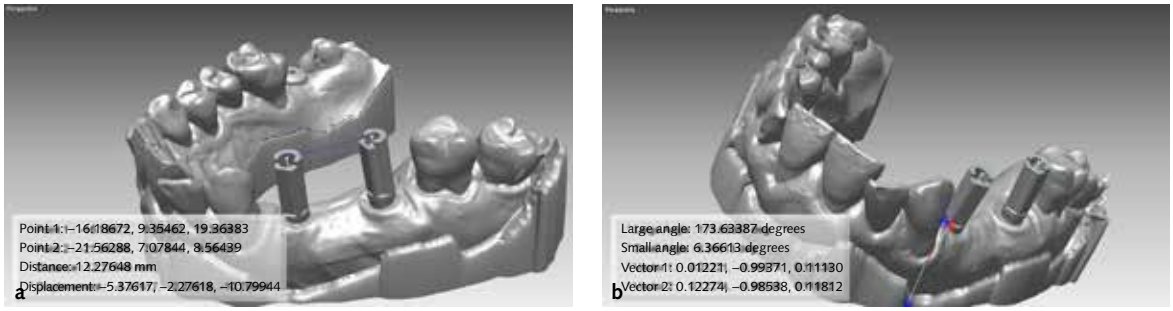

Figs 5a-b Measurement of **(a)** interimplant distance and **(b)** interimplant angulation between scan bodies using reverse engineering software.

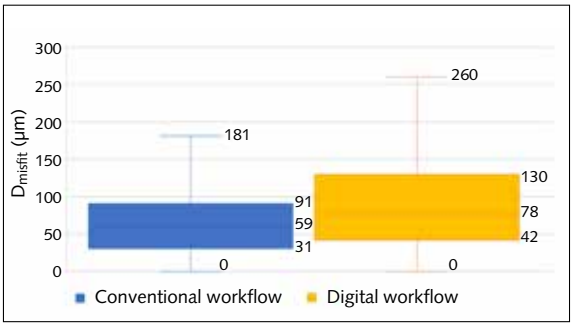

Fig 6 Median, IQR and minimum and maximum values for D_{misfit}.

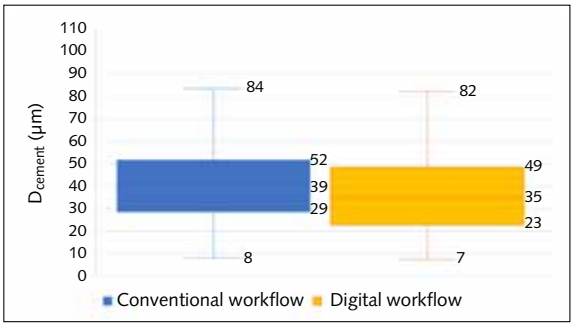

Fig 7 Median, IQR and minimum and maximum values for D_{cement}.

Table 1 Medians and IQR of D_{misfit} and D_{cement} in zirconia FPDs supported by two implants in groups C and D

Values	Group C	Group D	*P* value (Wilcoxon signed-rank test)
D_{misfit} [IQR], µm	59.00 [60.00]	78.00 [88.00]	0.00
D_{cement} [IQR], µm	38.90 [23.20]	34.90 [25.70]	0.00

were correlated to the D_{misfit}, D_{cement}, ΔD_{misfit} and ΔD_{cement} data sets.

Statistical analysis was completed with R software (version 2.3-2, R Foundation for Statistical Computing, Vienna, Austria). A Shapiro-Wilk normality test was used to analyse the distribution of the data. Since the data were not normally distributed, non-parametric tests were used. A Wilcoxon signed-rank test for paired data and Friedman rank sum test were applied to compare the medians of the distances in the groups and subgroups for both workflows. A Spearman correlation test was used to estimate associations between D_{misfit}, ΔD_{misfit}, D_{cement} and ΔD_{cement} parameters and angulation of and distance between implants. G*Power (version 3.1.9.2, Dusseldorf University, Dusseldorf, Germany) was used to calculate the statistical power. Statistical significance was set at $P < 0.05$.

Results

The median, interquartile range (IQR) and minimum and maximum values for both groups are presented in Figs 6 and 7. According to the results of the Wilcoxon signed-rank test, D_{misfit}

Table 2 Comparison of D_{misfit} measurements in groups C and D

Measurement location	Group C	Group D	*P* value (Wilcoxon signed-rank test)	*P* value (Friedman rank sum test)
	Median [IQR], µm	Median [IQR], µm		
MB	51.50 [55.25]	65.00 [67.50]	0.00	0.01
ML	62.00 [58.50]	96.00 [93.00]	0.00	
DB	67.00 [61.75]	78.00 [73.75]	0.00	
DL	68.00 [72.00]	71.00 [101.25]	0.01	

Table 3 Comparison of D_{cement} measurements in groups C and D

Measurement location	Group C	Group D	*P* value (Wilcoxon signed-rank test)	*P* value (Friedman rank sum test)
	Median [IQR], µm	Median [IQR], µm		
MB	36.40 [20.70]	40.05 [29.48]	0.51	0.79
ML	40.00 [23.50]	35.30 [26.80]	0.00	
DB	41.85 [21.50]	35.8 [23.68]	0.00	
DL	35.65 [26.28]	31.75 [22.50]	0.00	

Table 4 Comparison of ΔD_{misfit} and ΔD_{cement} between different subgroups: maxilla vs mandible and two-unit vs three-unit vs four-unit FPDs

Subgroup	ΔD_{misfit}			ΔD_{cement}		
	Median [IQR], µm	*P* value (Wilcoxon signed rank test)	*P* value (Friedman rank sum test)	Median [IQR], µm	*P* value (Wilcoxon signed rank test)	*P* value (Friedman rank sum test)
Maxilla (n = 14)	44.00 [64.00]	0.58	NR	18.00 [17.60]	0.00	NR
Mandible (n = 10)	42.50 [66.00]			13.70 [19.60]		
Two-unit (n = 7)	36.50 [47.25]	NR	0.47	14.70 [21.09]	NR	0.05
Three-unit (n = 11)	53.00 [72.00]			17.60 [17.70]		
Four-unit (n = 6)	42.50 [81.00]			14.65 [19.27]		

was higher in group D than in group C ($P < 0.05$) (Table 1). D_{misfit} measurements were found to be significantly different between groups C and D when analysing MB, ML, DB and DL measurement sites separately ($P < 0.05$) (Table 2). The cement gap (D_{cement}) was larger in group C ($P < 0.05$). According to the Friedman rank sum test, the D_{cement} measurements in the MB, ML, DB and DL sites were not significantly different between groups C and D ($P = 0.79$) (Table 3).

Comparisons of the ΔD_{misfit} values between the specimens from the maxilla and mandible showed that the differences were not significant ($P = 0.58$). ΔD_{misfit} was also not significantly different when comparing the two-, three- and four-unit FPDs ($P = 0.47$). Values for ΔD_{cement} were significantly different when comparing FPDs in the maxilla and mandible ($P < 0.05$); however, no difference was detected for ΔD_{cement} when comparing two-, three- and four-unit FPDs ($P = 0.05$) (Table 4).

A weak negative correlation was found between D_{misfit} and interimplant distance in group C (Table 5). In both groups, D_{cement} did not correlate significantly with interimplant distance or angulation.

Table 5 Spearman correlation coefficients between D_{misfit} (C), D_{misfit} (D), ΔD_{misfit} and ΔD_{cement} and mean interimplant distance and angulation

Variable	Interimplant distance	Interimplant angulation
D_{misfit} (group C)	–0.199	–0.040 (NS)
D_{misfit} (group D)	–0.094 (NS)	0.051 (NS)
D_{cement} (group C)	0.117 (NS)	0.097 (NS)
D_{cement} (group D)	0.115 (NS)	0.222 (NS)
ΔD_{misfit}	–0.034 (NS)	0.151 (NS)
ΔD_{cement}	–0.0136 (NS)	–0.036 (NS)

NS, not significant.

Discussion

Limited research is available on the accuracy outcomes with implant-supported prostheses fabricated using a digital workflow; however, in these studies, the fit was evaluated using mainly subjective and not standardised criteria[17]. In the present study, the fit and cement gap were assessed and compared for conventionally and digitally fabricated FPD bars supported by two implants using SEM measurements, and the fit of the FPD bars in both groups was appraised clinically.

The impression procedure is of critical importance when considering the overall accuracy of the workflow. Use of IOSs is becoming widespread in clinical practice, and it is claimed that they can achieve acceptable impression accuracy levels, with deviations smaller than 0.4 degrees for angulation[18,19] and less than 100 µm for linear measurements[20-22]. These results have mainly been reported in experimental studies, however, and thus cannot be directly extrapolated to the clinical field[23]. Many intraoral factors, such as movement of the patient and the soft tissues and tongue, can significantly affect the accuracy of digital impressions[24]. To address these factors in the present study, digital impressions were taken under clinical conditions.

Linear deviations between splinted conventional implant impressions and digital impressions have been found to vary from 11 µm in laboratory studies[19] to 130 µm in clinical studies[25]. One study reported better accuracy with digital impressions than with conventional ones[26]. Thus, it is hypothetically possible that the fit of FPDs produced using a digital workflow could be better than that achieved with conventionally fabricated FPDs[27]. However, there is still a lack of evidence to support the selection of digital impressions for multiple-unit implant prosthodontics. As such, conventional impressions are still considered the standard technique, especially for more complex cases. Unlike in laboratory studies, no true reference is available in clinical studies when comparing the accuracy of different impression techniques. During the present investigation, well verified master casts produced from splinted conventional implant impressions were considered as the reference.

Impression taking is just the first step in the workflow; thus, the accuracy of the final prosthesis will be influenced by the distortions that are generated during CAD/CAM and other subsequent fabrication steps. Distortions pertinent to the specific workflow can lead to incomplete seating of the prosthetic component. The design of the bar eliminated possible interference with proximal contacts and soft tissues, and the clinician's perception was therefore not affected by these factors.

Analysis of the SEM measurements showed that the median value for D_{misfit} in group D (78 µm) was significantly different to that for the C group (59 µm). To avoid the influence of confounding factors, CAD design, milling, sintering and other parameters and procedures were standardised. All clinical procedures were completed by one investigator (VG) and lab procedures by another (AG).

As misfit of 150 µm is widely reported as a clinical threshold[1], the 19-µm difference in median values of D_{misfit} between groups C and D could be considered to have limited clinical significance. However, this clinical threshold was exceeded when examining the maximum values in groups C and D (181 µm and 250 µm, respectively). Again, it must be noted that measurements were taken on a verified master cast that can deviate, even minimally, from the intraoral situation. As such, these results cannot be directly associated with the intraoral fit. Study designs that would be capable of obtaining reference data representing the intraoral situation are needed.

Significant differences were found between the D_{misfit} values for the different groups and locations.

D_{misfit} values up to 34 µm higher were recorded in group D considering the different locations. An increase in marginal discrepancy could lead to less passive restoration and less precise fit between the titanium base and the implant. An increase in bacterial contamination due to implant–abutment misfit can cause inflammatory complications[28] and have detrimental effects on implant and marginal bone stability[29]. The ability of the clinician to detect these misfits clinically remains questionable.

With a conventional workflow, milled restorations are usually cemented to titanium bases by finger pressure using the master cast. Although this is the standard procedure, the cementation of multiple-unit cases with angulated implants can be more challenging and can lead to less reliable cementation. Cementation on the master cast makes it possible to adjust restoration contours, as well as proximal and occlusal contacts; however, discrepancies caused by factors such as time-dependent cast distortion and repositioning accuracy of prosthetic components may lead to incomplete seating of the restoration on the titanium base and a less uniform cement gap.

3D printed models are still regarded as less accurate than conventional ones and can introduce significant deviations into the workflow[13,30,31]. If full-contour restorations are planned, a cast-free, fully digital workflow can be selected. In this case, the restorations are cemented to titanium bases without the 3D printed model. For this reason, a cast-free approach was chosen in the present study. The original non-hex titanium bases were cemented with resin cement according to the manufacturer's instructions, using a technique widely discussed in the literature[12,32].

Zirconia abutments bonded to titanium bases show similar mechanical stability compared with customised titanium abutments[33]. The size of the cement gap is essential for retention of the FPD on custom abutments or titanium bases. Mehl et al[34] reported that the resulting cement space should be tested before the workflow is established, and a cement space of around 60 µm is preferred over a space of 100 µm. Though D_{cement} was measured only on the marginal edge of the titanium base, it did not exceed 100 µm in either group (41.68 µm in group C and 36.45 µm in group D). However, the maximum D_{cement} values in both groups were slightly over 80 µm. The higher number of outliers in group C implies that the cementation technique on the master cast was less predictable in this regard. Seating of the restoration on the titanium bases is more difficult when there are high angulations between implants. Furthermore, it was difficult to standardise the pressure applied by the dental technician during cementation of the zirconia bars in both groups. These aspects could potentially affect the cement gap.

Centring of the titanium abutment in the zirconia coping during cementation is vital for retention of the restorations. To achieve an even distribution of cement, a proper fit of the restoration on the master cast with titanium bases attached to the implant analogues must first be achieved. In the present study, no statistically significant differences in D_{cement} were found between the measurements at different locations ($P = 0.79$) in both groups. It can therefore be claimed that cement distribution between the bar and titanium base was even at the margins circumferentially. However, the present study did not evaluate the cement thickness on the axial walls of the titanium bases.

Better seating of the restoration on a titanium base was found in group D since the base could adopt a position of maximum congruency to the zirconia framework without any restrictions; however, this had a negative impact on the fit as D_{misfit} was 19 µm higher in group D. Future studies should examine whether an increase in the cement gap or misfit would have a more significant effect on the long-term prognosis of implant-supported FPDs. Other studies have shown that reliability of cementation was also affected by the type of cement, surface preparation, thermocycling, fatigue simulation and prosthesis material[32,34].

The fit of a restoration can be influenced by the clinical situation, with distance, angulation and depth of the implant placement considered important factors. The length of the prosthesis and its curvature along the jaw can also affect the final fit[3,10]. In the present study, two-, three- and four-unit restorations were all placed in the posterior region. However, neither ΔD_{misfit} ($P = 0.47$) nor

ΔD_{cement} ($P = 0.05$) showed statistically significant differences between the different lengths of the restorations. ΔD_{misfit} of the maxillary and mandibular restorations was also not statistically significant ($P = 0.58$), which implies that the vertical fit of the restorations was not influenced by the length or location of the FPDs supported by two implants. However, a significant difference in ΔD_{cement} (4 µm) was recorded in the maxilla and mandible. This difference might have resulted from the tendency towards higher implant angulation in the premolar region. However, the clinical significance of this is questionable. Only one significant correlation between the measured variables and interimplant distance or angulation was found: a weak negative correlation between D_{misfit} and interimplant distance. A larger sample size is required to further clarify these correlations.

The limitations of the present study that may have affected the results must be discussed. It is highly possible that the results would not have been the same if a different IOS and conventional impression and master cast fabrication technique and different CAD/CAM settings and zirconia materials had been used. Moreover, standardised zirconia bars were used for evaluation rather than completed restorations in the present study. The amount of ceramic layering, different layering temperatures and final clinical proximal and occlusal contact adjustment could thus affect the results in clinical practice[35].

The present results are specific to the implant–abutment connection used in this study. Use of hex or non-hex components could affect the fit of the implant-supported FPD. Different outcomes should also be expected with multi-unit abutment-level prosthetic procedures. It was demonstrated that an external abutment connection could better prevent vertical displacement during screw tightening; thus, larger vertical displacement occurs with internal types of implant–abutment connection[36]. Moreover, non-original prosthetic components can be associated with lower internal accuracy[37] and influence the fit of the prosthesis.

An attempt was made to evaluate the clinical fit of the FPD bars in groups C and D in a consistent way. However, detecting misfit by applying alternate finger pressure and using the Sheffield test are regarded as subjective procedures and lack reliability.

Conclusions

Within the limitations of this study, it can be concluded that the fit and cement gap of zirconia FPD bars supported by two implants made using conventional and digital workflows differed significantly, with the conventional workflow resulting in a better fit and the digital workflow producing a smaller cement gap. Nevertheless, the reported differences were minor, and of limited clinical significance. A cast-free digital workflow can be regarded as a clinically viable treatment modality. The fit and cement gap were not associated with the length of the implant-supported FPD bar or the angulation between implants. Further studies are required to establish objective clinical criteria to detect the misfit of screw-retained implant-supported FPDs.

Acknowledgements

The authors thank dental CAD/CAM specialist Tomas Simonaitis (Digitorum Lab) for preparing the study specimens.

References

1. Jemt T. Failures and complications in 391 consecutively inserted fixed prostheses supported by Brånemark implants in edentulous jaws: A study of treatment from the time of prosthesis placement to the first annual checkup. Int J Oral Maxillofac Implants 1991;6:270–276.
2. Abduo J, Bennani V, Waddell N, Lyons K, Swain M. Assessing the fit of implant fixed prostheses: A critical review. Int J Oral Maxillofac Implants 2010;25:506–515.
3. Katsoulis J, Takeichi T, Sol Gaviria A, Peter L, Katsoulis K. Misfit of implant prostheses and its impact on clinical outcomes. Definition, assessment and a systematic review of the literature. Eur J Oral Implantol 2017;10(Suppl 1):121–138.
4. Kan JY, Rungcharassaeng K, Bohsali K, Goodacre CJ, Lang BR. Clinical methods for evaluating implant framework fit. J Prosthet Dent 1999;81:7–13.
5. Sahin S, Cehreli MC. The significance of passive framework fit in implant prosthodontics: Current status. Implant Dent 2001;10:85–92.

6. Papaspyridakos P, Chen CJ, Gallucci GO, Doukoudakis A, Weber HP, Chronopoulos V. Accuracy of implant impressions for partially and completely edentulous patients: A systematic review. Int J Oral Maxillofac Implants 2014;29:836–845.
7. Siadat H, Beyabanaki E, Mousavi N, Alikhasi M. Comparison of fit accuracy and torque maintenance of zirconia and titanium abutments for internal tri-channel and external-hex implant connections. J Adv Prosthodont 2017;9:271–277.
8. Alikhasi M, Siadat H, Nasirpour A, Hasanzade M. Three-dimensional accuracy of digital impression versus conventional method: Effect of implant angulation and connection type. Int J Dent 2018;2018:3761750.
9. Alonso-Pérez R, Bartolomé JF, Ferreiroa A, Salido MP, Pradíes G. Original vs. non-original abutments for screw-retained single implant crowns: An in vitro evaluation of internal fit, mechanical behaviour and screw loosening. Clin Oral Implants Res 2018;29:1230–1238.
10. Abduo J. Fit of CAD/CAM implant frameworks: A comprehensive review. J Oral Implantol 2014;40:758–766.
11. Semper-Hogg W, Kraft S, Stiller S, Mehrhof J, Nelson K. Analytical and experimental position stability of the abutment in different dental implant systems with a conical implant-abutment connection. Clin Oral Investig 2013;17:1017–1023.
12. Arce C, Lawson NC, Liu PR, Lin CP, Givan DA. Retentive force of zirconia implant crowns on titanium bases following different surface treatments. Int J Oral Maxillofac Implants 2018;33:530–535.
13. Revilla-León M, Gonzalez-Martín Ó, Pérez López J, Sánchez-Rubio JL, Özcan M. Position accuracy of implant analogs on 3D printed polymer versus conventional dental stone casts measured using a coordinate measuring machine. J Prosthodont 2018;27:560–567.
14. Pan S, Guo D, Zhou Y, Jung RE, Hämmerle CHF, Mühlemann S. Time efficiency and quality of outcomes in a model-free digital workflow using digital impression immediately after implant placement: A double-blind self-controlled clinical trial. Clin Oral Implants Res 2019;30:617–626.
15. Rutkūnas V, Gečiauskaitė A, Jegelevičius D, Vaitiekūnas M. Accuracy of digital implant impressions with intraoral scanners. A systematic review. Eur J Oral Implantol 2017; 10(Suppl 1):101–120.
16. Rutkūnas V, Ignatovic J. A technique to splint and verify the accuracy of implant impression copings with light-polymerizing acrylic resin. J Prosthet Dent 2014;111: 254–256.
17. Cappare P, Sannino G, Minoli M, Montemezzi P, Ferrini F. Conventional versus digital impressions for full arch screw-retained maxillary rehabilitations: A randomized clinical trial. Int J Environ Res Public Health 2019;16:829.
18. Mangano FG, Veronesi G, Hauschild U, Mijiritsky E, Mangano C. Trueness and precision of four intraoral scanners in oral implantology: A comparative in vitro study. PloS One 2016;11:e0163107.
19. Gherlone E, Capparé P, Vinci R, Ferrini F, Gastaldi G, Crespi R. Conventional versus digital impressions for "all-on-four" restorations. Int J Oral Maxillofac Implants 2016;31:324–330.
20. Chew AA, Esguerra RJ, Teoh KH, Wong KM, Ng SD, Tan KB. Three-dimensional accuracy of digital implant impressions: Effects of different scanners and implant level. Int J Oral Maxillofac Implants 2017;32:70–80.
21. Gimenez-Gonzalez B, Hassan B, Özcan M, Pradíes G. An in vitro study of factors influencing the performance of digital intraoral impressions operating on active wavefront sampling technology with multiple implants in the edentulous maxilla. J Prosthodont 2017;26:650–655.
22. Gintaute A. Accuracy of Computerized and Conventional Impression-making Procedures of Straight and Tilted Dental Implants [thesis]. Freiburg: Albert-Ludwigs-Universität, 2015.
23. Flügge T, van der Meer WJ, Gonzalez BG, Vach K, Wismeijer D, Wang P. The accuracy of different dental impression techniques for implant-supported dental prostheses: A systematic review and meta-analysis. Clin Oral Implants Res 2018;29(Suppl 16):374–392.
24. Gedrimiene A, Adaskevicius R, Rutkūnas V. Accuracy of digital and conventional dental implant impressions for fixed partial dentures: A comparative clinical study. J Adv Prosthodont 2019;11:271–279.
25. Alsharbaty MHM, Alikhasi M, Zarrati S, Shamshiri AR. A clinical comparative study of 3-dimensional accuracy between digital and conventional implant impression techniques. J Prosthodont 2019;28:e902–e908.
26. Menini M, Setti P, Pera F, Pera P, Pesce P. Accuracy of multi-unit implant impression: Traditional techniques versus a digital procedure. Clin Oral Investig 2018;22:1253–1262.
27. Nedelcu R, Olsson P, Nyström I, Thor A. Finish line distinctness and accuracy in 7 intraoral scanners versus conventional impression: An in vitro descriptive comparison. BMC Oral Health 2018;18:27.
28. Zekiy AO, Makurdumyan DA, Matveeva EA, Bogatov EA, Kaliiants TV. Antiseptic sealant and a nanocoated implant-abutment interface improve the results of dental implantation. Clin Implant Dent Relat Res 2019;21: 938–945.
29. Toia M, Stocchero M, Jinno Y, et al. Effect of misfit at implant-level framework and supporting bone on internal connection implants: Mechanical and finite element analysis. Int J Oral Maxillofac Implants 2019;34:320–328.
30. Cho SH, Schaefer O, Thompson GA, Guentsch A. Comparison of accuracy and reproducibility of casts made by digital and conventional methods. J Prosthet Dent 2015;113:310–315.
31. Jang Y, Sim JY, Park JK, Kim WC, Kim HY, Kim JH. Evaluation of the marginal and internal fit of a single crown fabricated based on a three-dimensional printed model. J Adv Prosthodont 2018;10:367–373.
32. Lopes ACO, Machado CM, Bonjardim LR, et al. The effect of CAD/CAM crown material and cement type on retention to implant abutments. J Prosthodont 2019;28: e552–e556.
33. Pitta J, Hicklin SP, Fehmer V, Boldt J, Gierthmuehlen PC, Sailer I. Mechanical stability of zirconia meso-abutments bonded to titanium bases restored with different monolithic all-ceramic crowns. Int J Oral Maxillofac Implants 2019;34:1091–1097.
34. Mehl C, Zhang Q, Lehmann F, Kern M. Retention of zirconia on titanium in two-piece abutments with self-adhesive resin cements. J Prosthet Dent 2018;120:214–219.
35. Yilmaz B, Alshahrani FA, Kale E, Johnston WM. Effect of feldspathic porcelain layering on the marginal fit of zirconia and titanium complete-arch fixed implant-supported frameworks. J Prosthet Dent 2018;120:71–78.
36. Kim SJ, Son K, Lee KB. Digital evaluation of axial displacement by implant-abutment connection type: An in vitro study. J Adv Prosthodont 2018;10:388–394.
37. Alonso-Pérez R, Bartolomé JF, Ferreiroa A, Salido MP, Pradíes G. Original vs. non-original abutments for screw-retained single implant crowns: An in vitro evaluation of internal fit, mechanical behaviour and screw loosening. Clin Oral Implants Res 2018;29:1230–1238.

Vygandas Rutkūnas

Vygandas Rutkūnas, qualification suffixes
Professor, Department of Prosthodontics, Institute of Odontology, Faculty of Medicine, Vilnius University, Vilnius, Lithuania.

Agne Gedrimiene, qualification suffixes
PhD Student, Department of Prosthodontics, Institute of Odontology, Faculty of Medicine, Vilnius University, Vilnius, Lithuania

Reinhilde Jacobs, qualification suffixes
Author title, OMFS IMPATH Research Group, Department of Imaging and Pathology, Faculty of Medicine, University of Leuven, Leuven, Belgium; Author title, Department of Oral and Maxillofacial Surgery, University Hospitals Leuven, Leuven, Belgium; Author title, Department of Dental Medicine, Karolinska Institutet, Huddinge, Sweden

Mangirdas Malinauskas, qualification suffixes
Author title, Laser Research Center, Vilnius University, Vilnius, Lithuania

Correspondence to:
Mrs Agne Gedrimiene, Department of Prosthodontics, Institute of Odontology, Faculty of Medicine, Vilnius University, Zalgirio g. 115, Vilnius, LT-08217 Lithuania. Email: geciauskaite.agne@gmail.com